Overview of ASDEX Upgrade Results

Ulrich Stroth

for the ASDEX Upgrade Team

Max-Planck-Institut für Plasmaphysik
D-85748 Garching

Presented at the FEC, San Diego 09.10.2012

AUG Program in preparation of ITER and DEMO

- Develop integrated scenarios for long-pulse operation of burning plasmas in ITER and DEMO including solutions for
  - plasma shaping
  - confinement and stability
  - divertor and exhaust
  - materials for divertor and the first wall

- Advance the physical understanding of related fundamental problems in order to create
  - reliable predicting capabilities
  - discover new paths to advanced plasma operation

- Educate young scientists and engineers that will run ITER

AUG Program in Preparation of ITER and DEMO

- To reach these goals, ASDEX Upgrade is a flexible device with versatile heating systems and excellent diagnostics:
  - closed divertor design
  - ITER-like plasma shape
  - full tungsten wall
  - mitigation scenarios for ELMs, power loads, NTMs, disruptions

- Here we present recent results on
  - high performance scenarios
  - ELM mitigation
  - Core and edge turbulent transport
  - H-mode physics
  - Divertor physics

Improved installations and control on ASDEX Upgrade

- Progress in real-time feed-back control of
  - Divertor power load → dual radiative cooling
  - Plasma position → reflectometry on HFS and LFS
  - Neocl. tearing modes → detection, beam tracing, ECRH launch control
  - Disruptions → massive gas injection with multiple valves

A. Kallenbach EPS 2012

J. Santos NF 2012

M. Reich EPS 2012

G. Pautasso EPS 2012

- Magnetic perturbation coils for ELM suppression

W. Suttrop EX/3-4

- Heating and current drive
  - ECRH power upgraded to 4 MW
  - ICRH (6 MW) with broader antenna limiter partly boron coated
  - NBI power of 20 MW

J. Stober EX/1-4

V. Bobkov EX/5-19

ASDEX Upgrade tungsten wall and perturbation coils

- R = 1.65 m, a = 0.5 m, B_{tor} = 2.5 T, I_P = 1.2 MA, P_{tot} = 24 MW

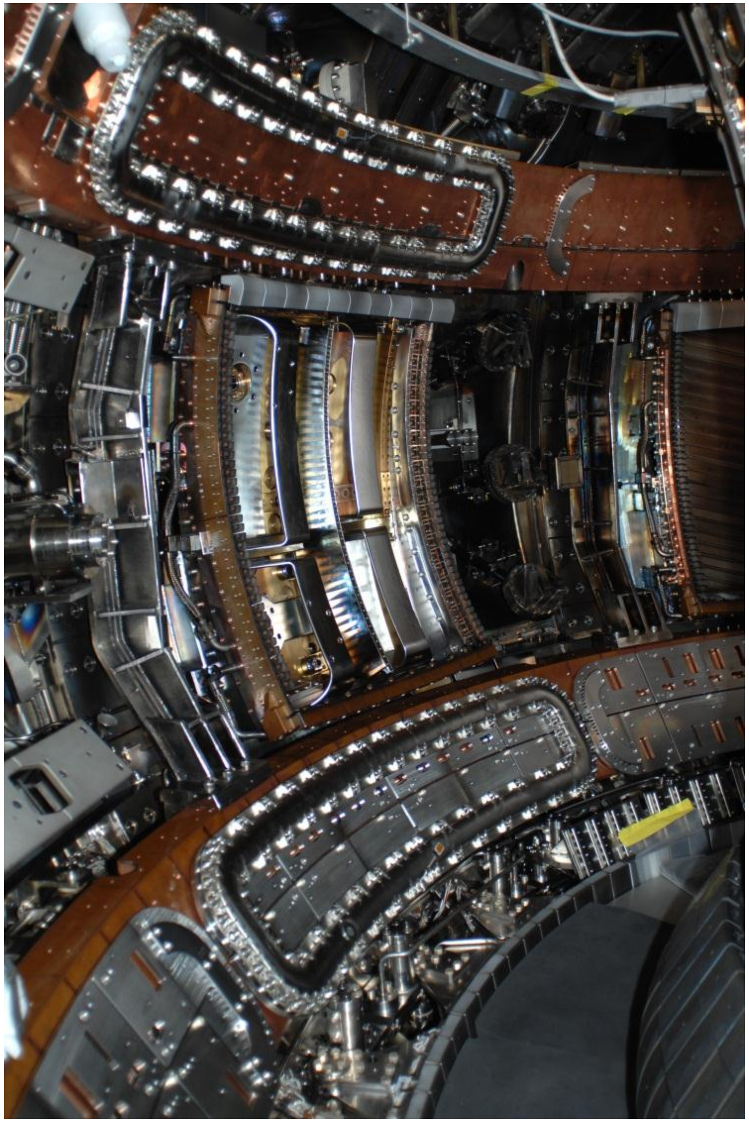

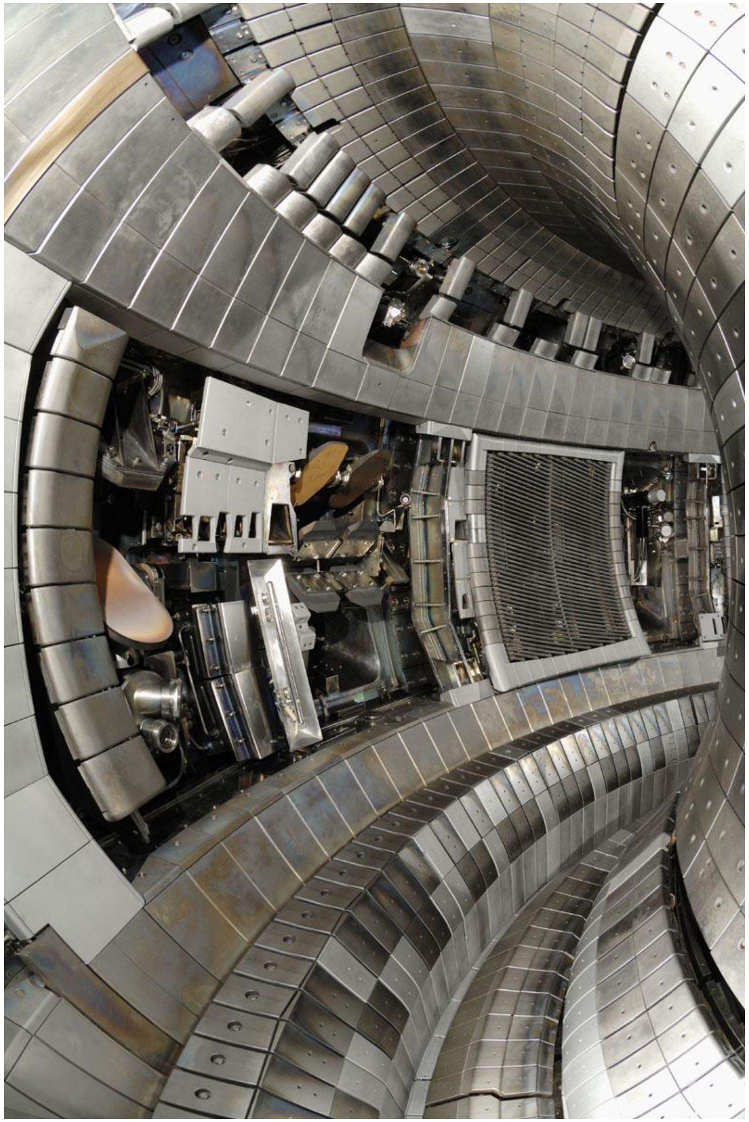

High performance discharges with *P*/*R* = 14 MW/m

- NBI+ECRH+ICRH of 23 MW with nitrogen cooling to limit the power load

A. Kallenbach EPS 2012

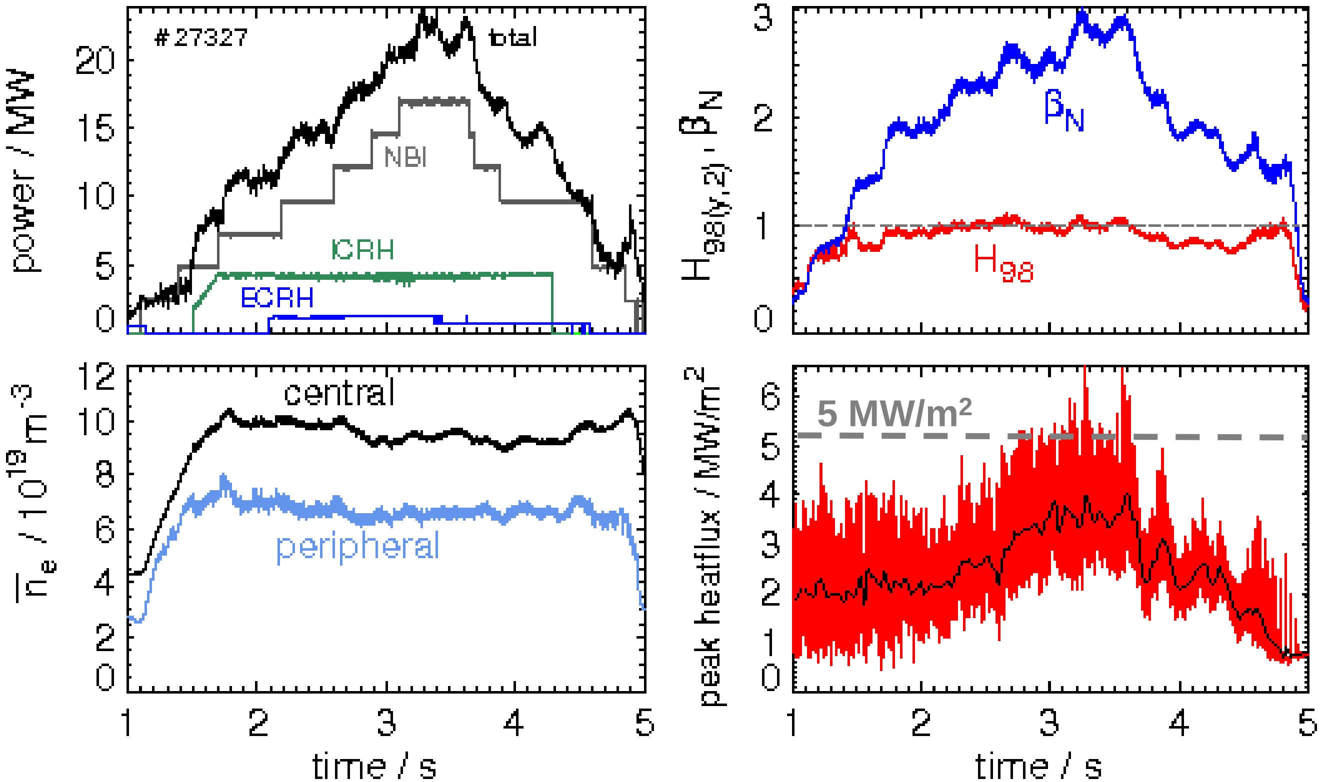

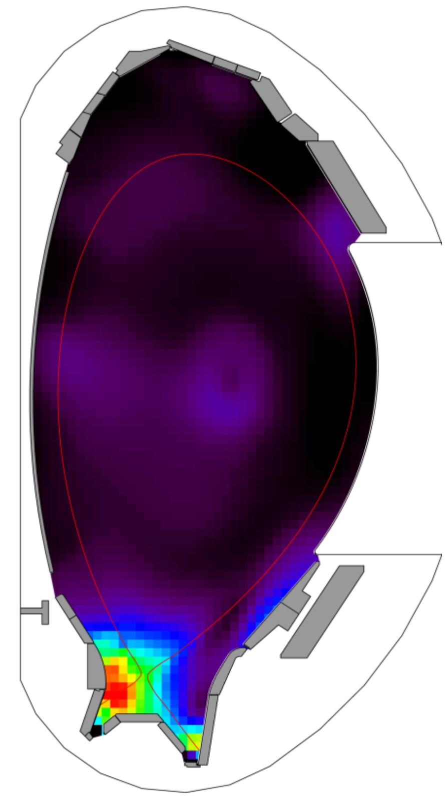

- Total radiated power: 20 MW
- Divertor heat load < 5 MW/m² at H ≈ 1; β_N ≈ 2.8
- Divertor radiation: 9 MW → well above L-H threshold
- 4 MW ICRH: progress on ICRH compatibility with the W wall

V. Bobkov EX/5-19

High performance discharges with *P*/*R* = 14 MW/m

- NBI+ECRH+ICRH of 23 MW
- Dual radiation feedback control
  - Argon for core radiation (feedback on bolometry)
  - Nitrogen for divertor radiation (T_{div} or bolometry)
  - $Z_{eff} = 2$, $c_W = 2\cdot10^{-5}$, $c_{Ar} \leq 3\cdot10^{-3}$
- Core radiation: 15 MW (67%)
  - Close to P_{thres} at H = 1, $\beta_N = 3$
- Divertor radiation 5 MW
- Peak heat flux < 5 MW/m^2
- Higher *P*/*R* values are possible → important for DEMO

A. Kallenbach ITR/1-1

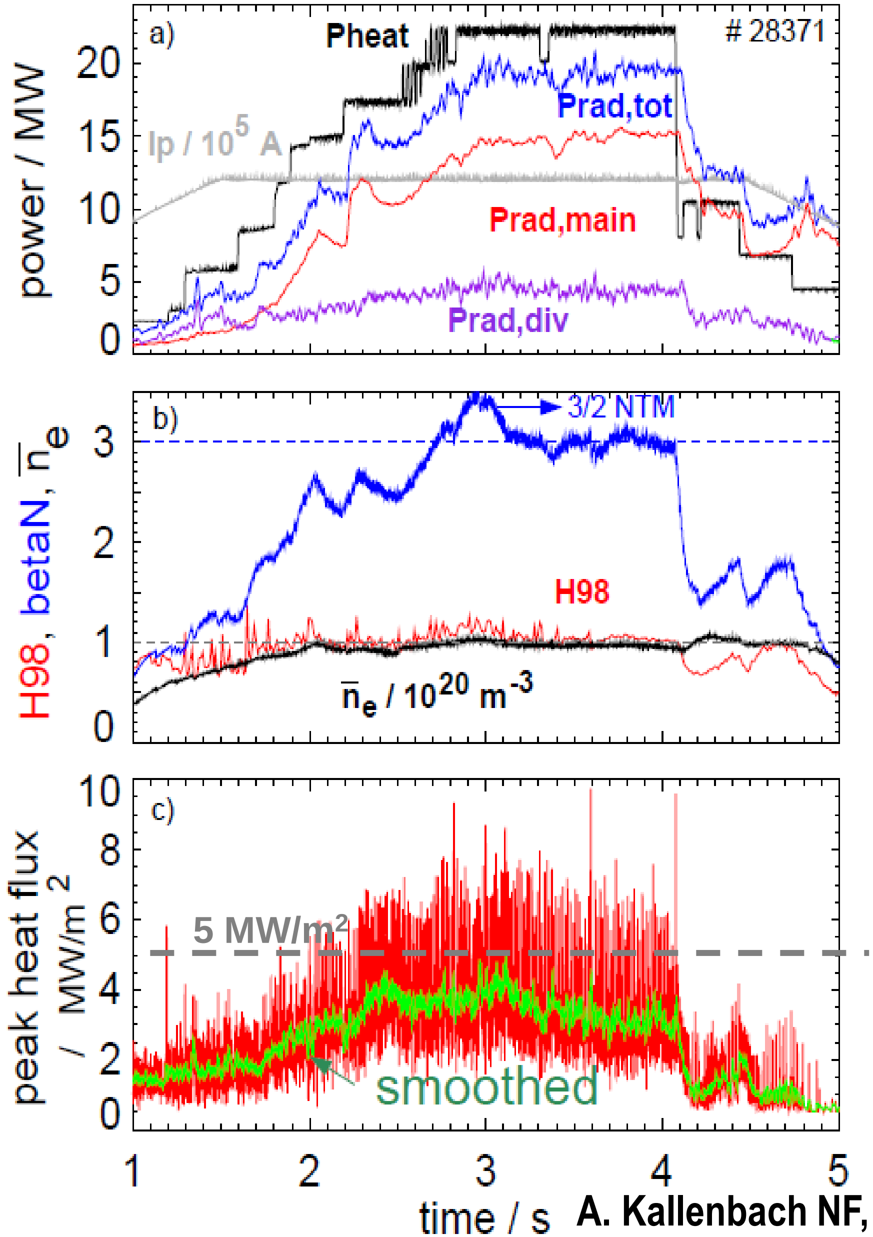

A. Kallenbach NF, sub.

ELM mitigation by magnetic perturbation coils

- Type-I ELMy H-modes
- Robust ELM suppression at high density (> 0.6 n_{GW})
- ELMs are replaced by small MHD events

- ELM mitigation independent of
  - heating method
  - safety factor *q*
  - coils phasing (res./non-res.)

W. Suttrop EX/3-4

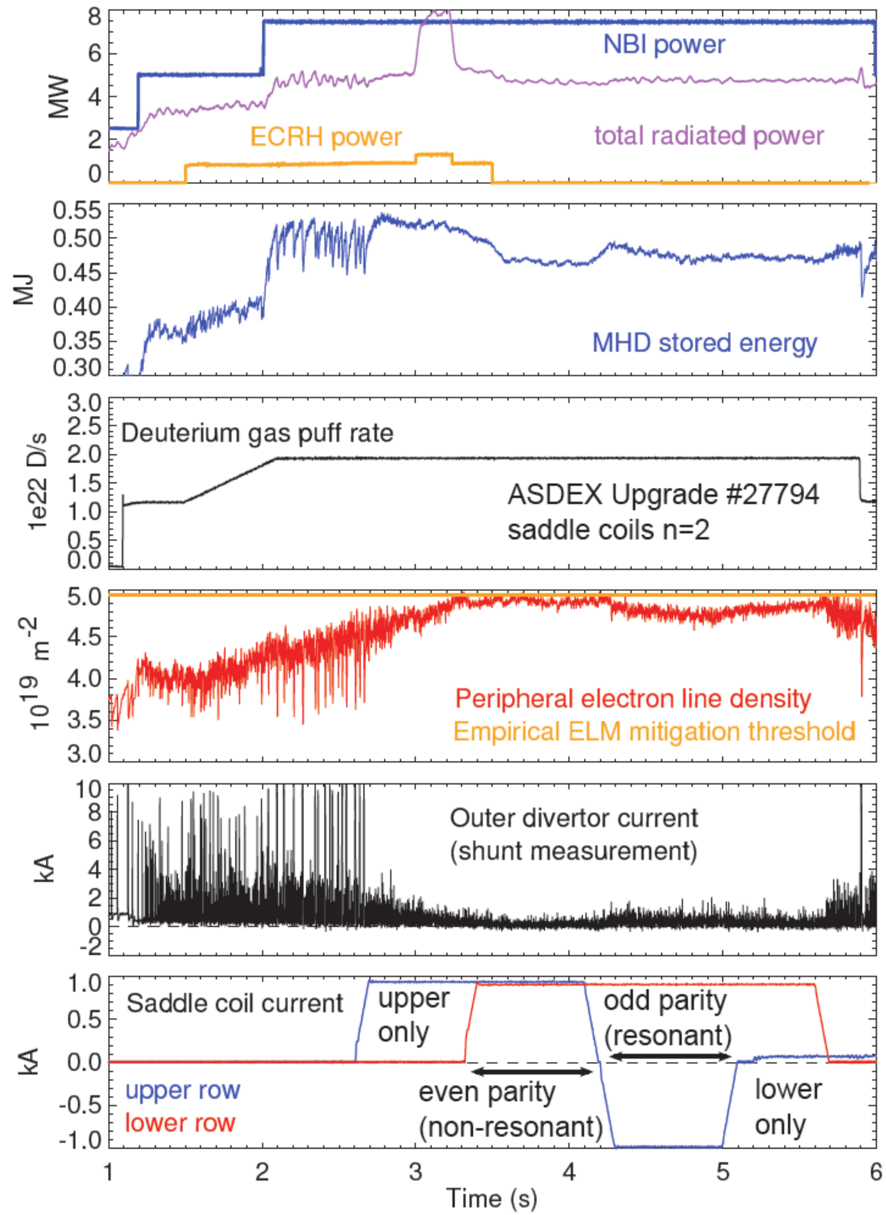

ELM mitigation by magnetic perturbation coils

- Critical parameter

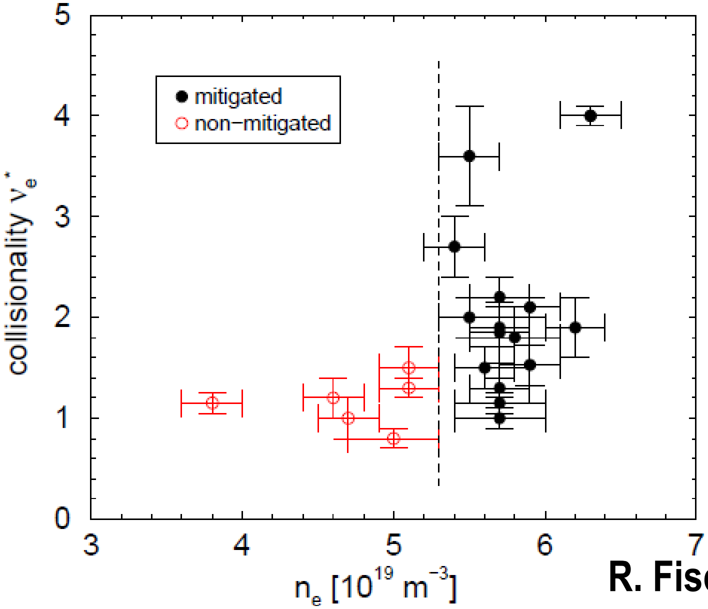

R. Fischer, PPCF 2012

- Mitigation
  - at high density not high collisionality
  - independent of toroidal flow

W. Suttrop EX/3-4

- Effect on profiles

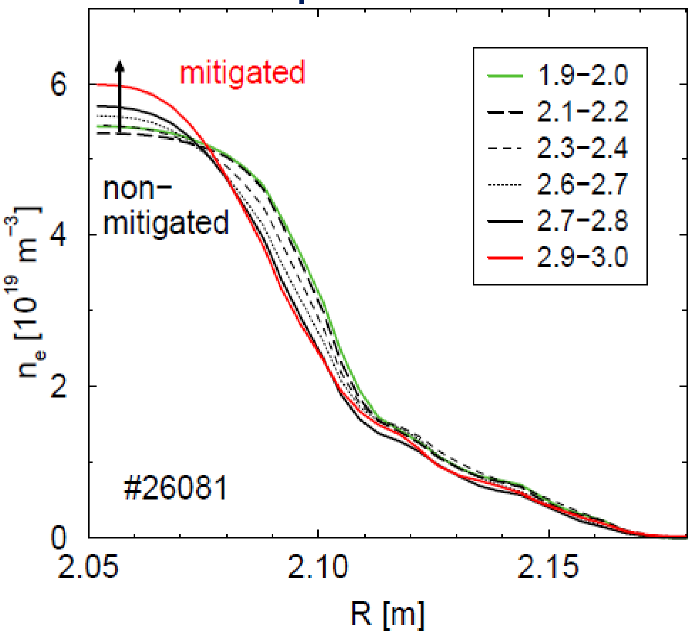

- Minor effect on
  - confinement
  - H-mode pedestal pressure
  - existing MHD modes
- Stronger effect seen at low density and *q*

M. Garcia-Munoz EX/P6-03

Influence of perturbation coils on divertor power load

- Thermography on divertor targets

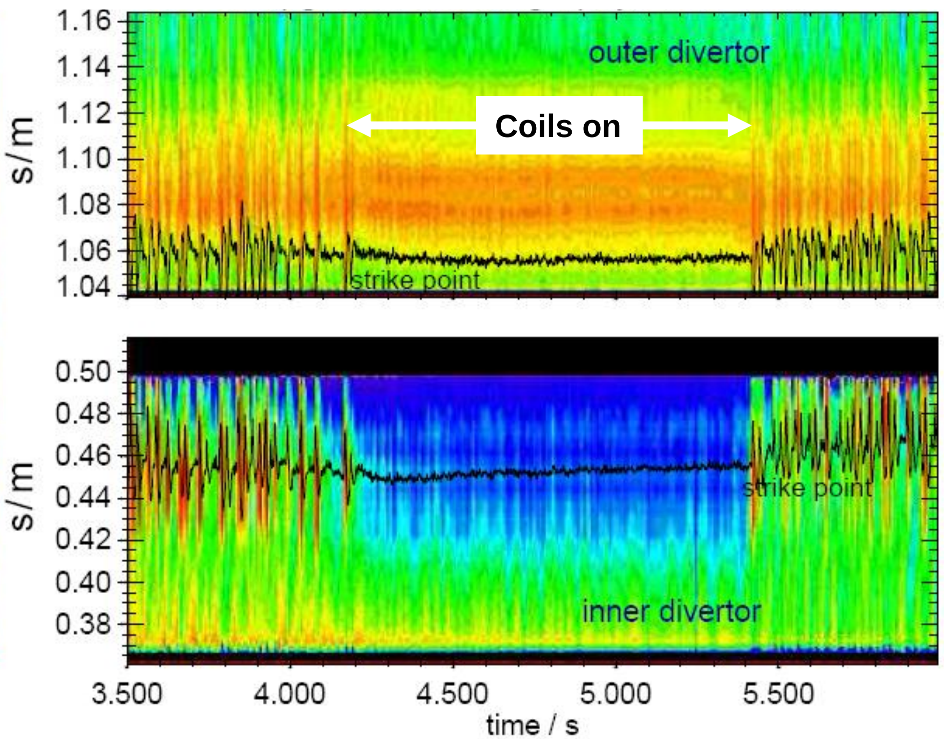

- Reduced peak power load
- Strike line splits up
- Agreement with EMC3 vacuum-field calculation

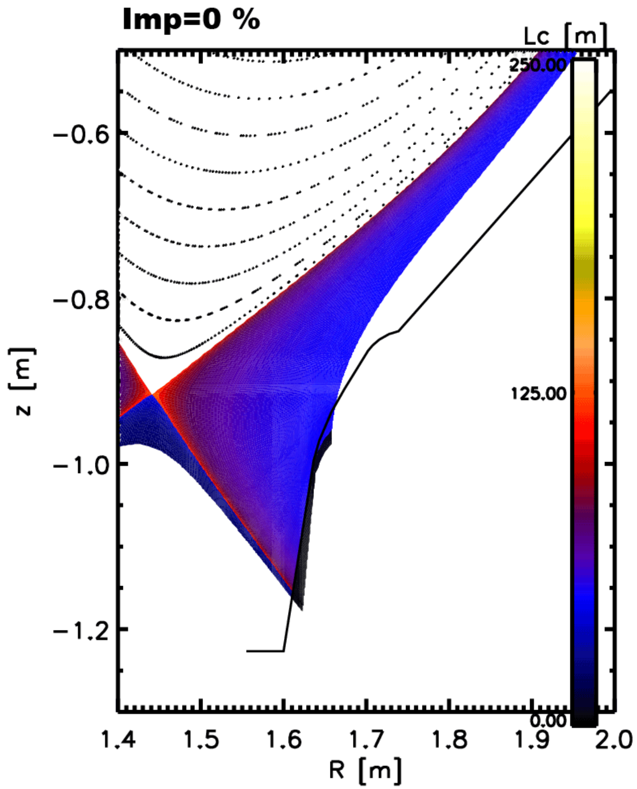

T. Lunt, NF 2012

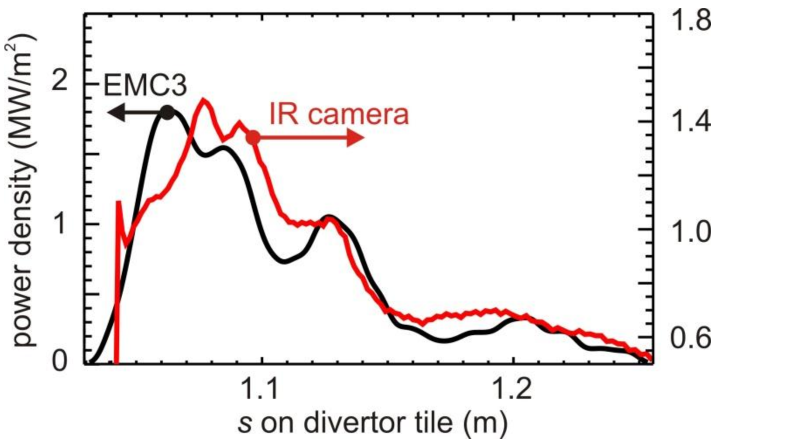

Enhanced pellet fuelling efficiency without ELMs

- H-modes with n/n_{GW} = 1.5 have been obtained

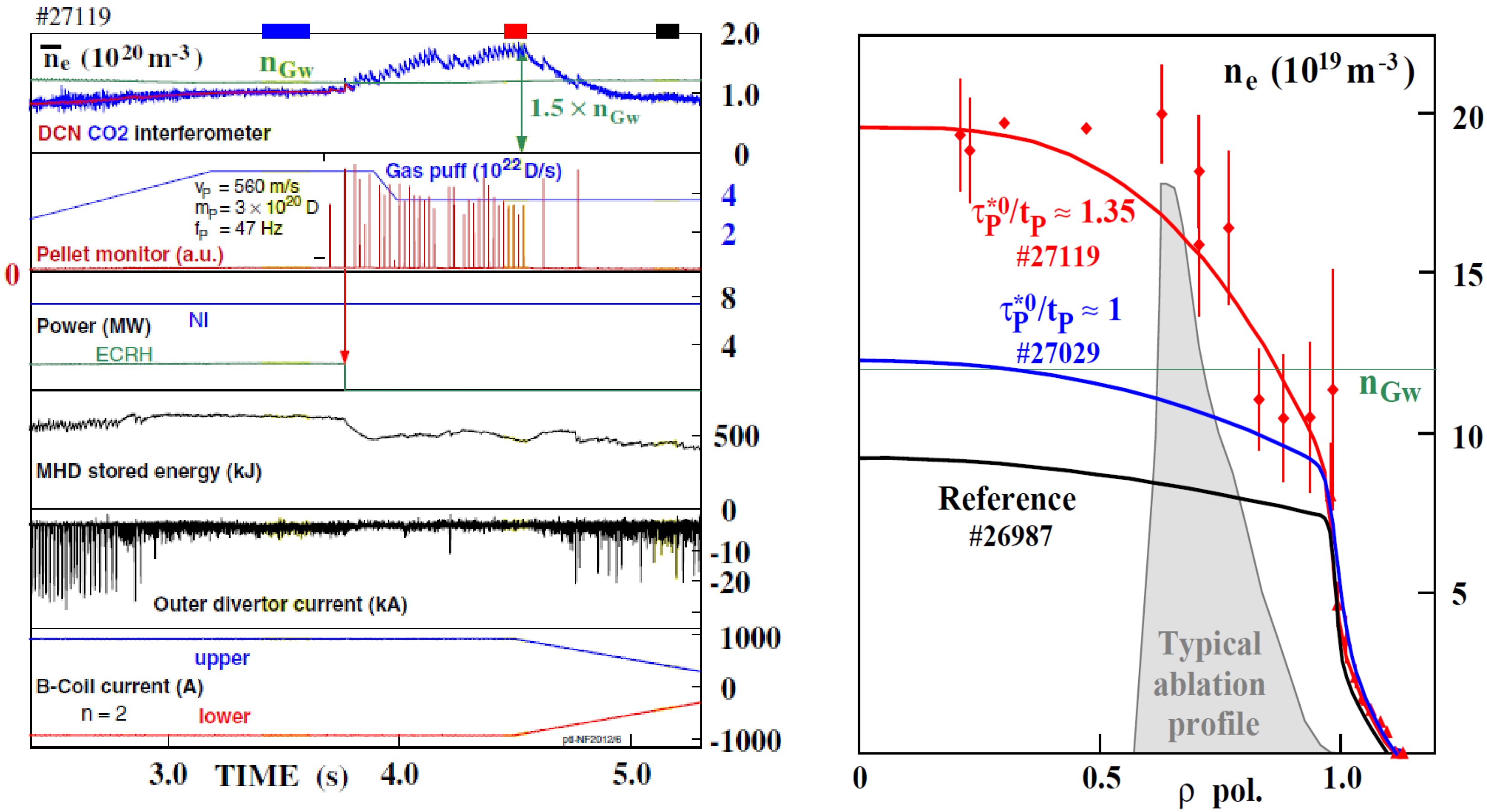

- Very efficient fuelling with HFS pellet injection and suppressed ELMs
- Edge density is at n/n_{GW} = 0.9

P. Lang EX/P4-01

Plasma rotation at zero external momentum input

- CXRS toroidal rotation database
  - OH, ECRH and ICRH
  - L- and H-mode

- Core rotation shows
  - strong variation incl. reversal
  - correlation with velocity gradient
  - similar behavior regardless of confinement regime

- Rotation gradient and density gradient are correlated
  - peaked density profiles appear with flat to hollow rotation profiles

R. McDermott EX/2-1

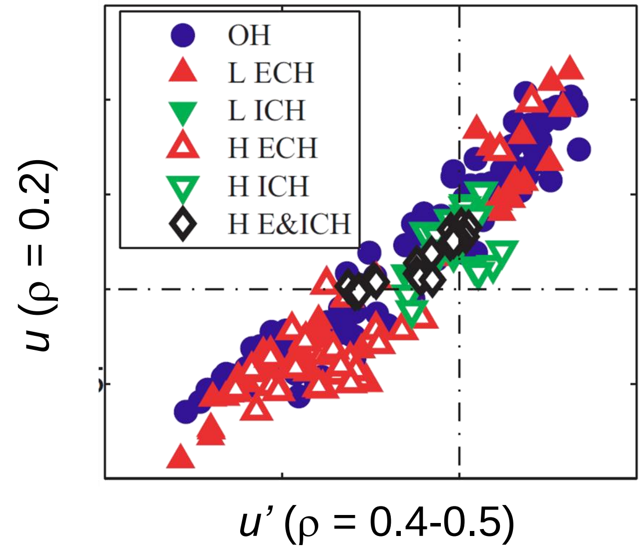

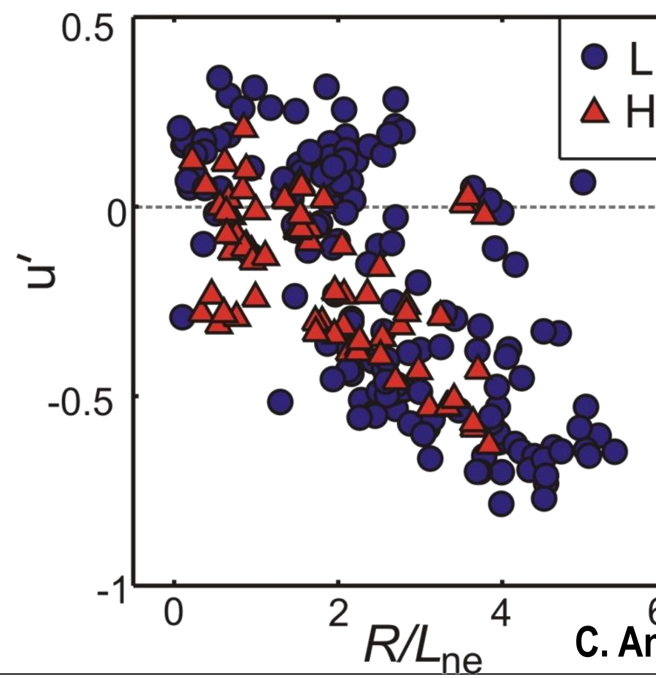

C. Angioni PRL 11

Residual stress drives core toroidal rotation

- Gyro-kinetic calculations (GS2)
  $\rightarrow$ density peaking depends on collisionality (TEM vs. ITG)

  E. Fable PPCF 2010

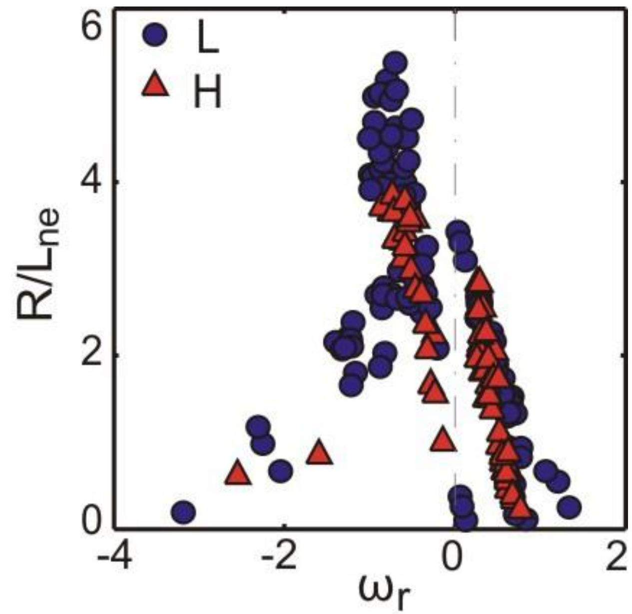

- Density gradient is dominant term in residual stress

- Local linear gyro-kinetic simulation (tilt angle -0.3) correctly captures L_n/r dependence of toroidal flow

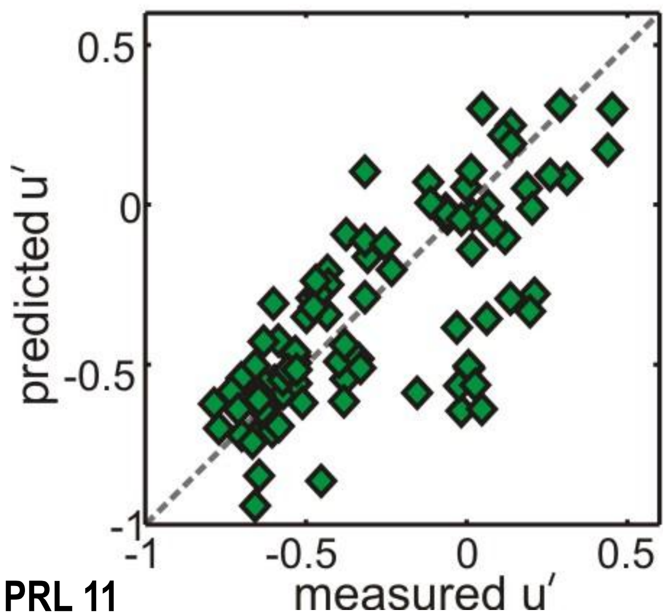

- ECRH $\rightarrow$ collisionality $\rightarrow$ turbulence regime $\rightarrow$ density peaking $\rightarrow$ plasma rotation

R. McDermott EX/2-1

C. Angioni PRL 11

Residual stress in combined ECRH + NBI discharges

- Addition of ECRH peaks density and flattens rotation profile

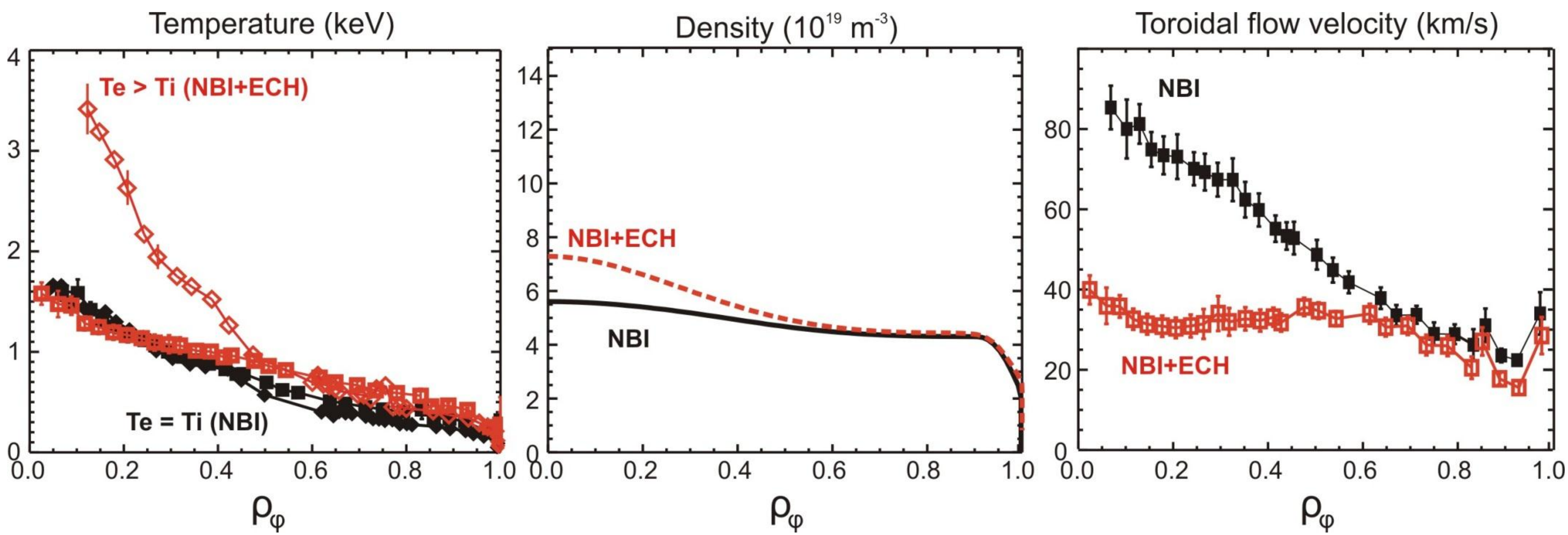

R. McDermott PPCF 2011

- ECRH drives transition from ITG to TEM
- Consistent with density-gradient dependence of the residual stress

R. McDermott EX/2-1

Fast-ion slowing down and diffusion are classical

- Consistent modeling of the entire D_α spectrum using TRANSP and virtual diag. (no free parameter)

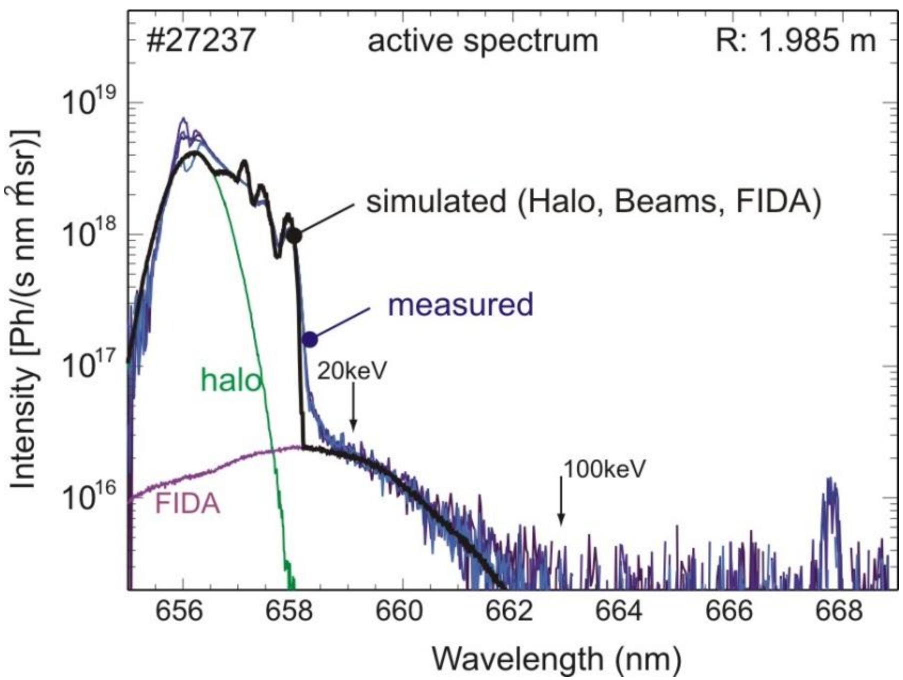

- Extract CX emission from fast ions (FIDA) due to NBI

B. Geiger EPS 2012

- Radial FIDA intensity profiles from on/off-axis NBI

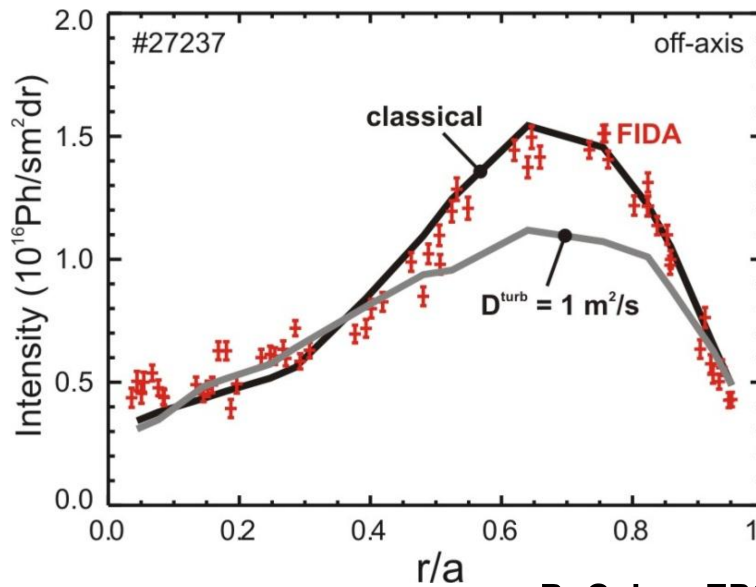

B. Geiger EPS 2012

  - agree with classical slowing down and diffusion
  - turbulent diffusion coefficient of 1 m²/s clearly ruled out

L-H transition studies

- Power threshold depends on density
- Tungsten wall: L-H threshold about 20% below scaling
- GAMs in L mode, flow-turbulence interactions in the I-phase
- I-phase extends to high density

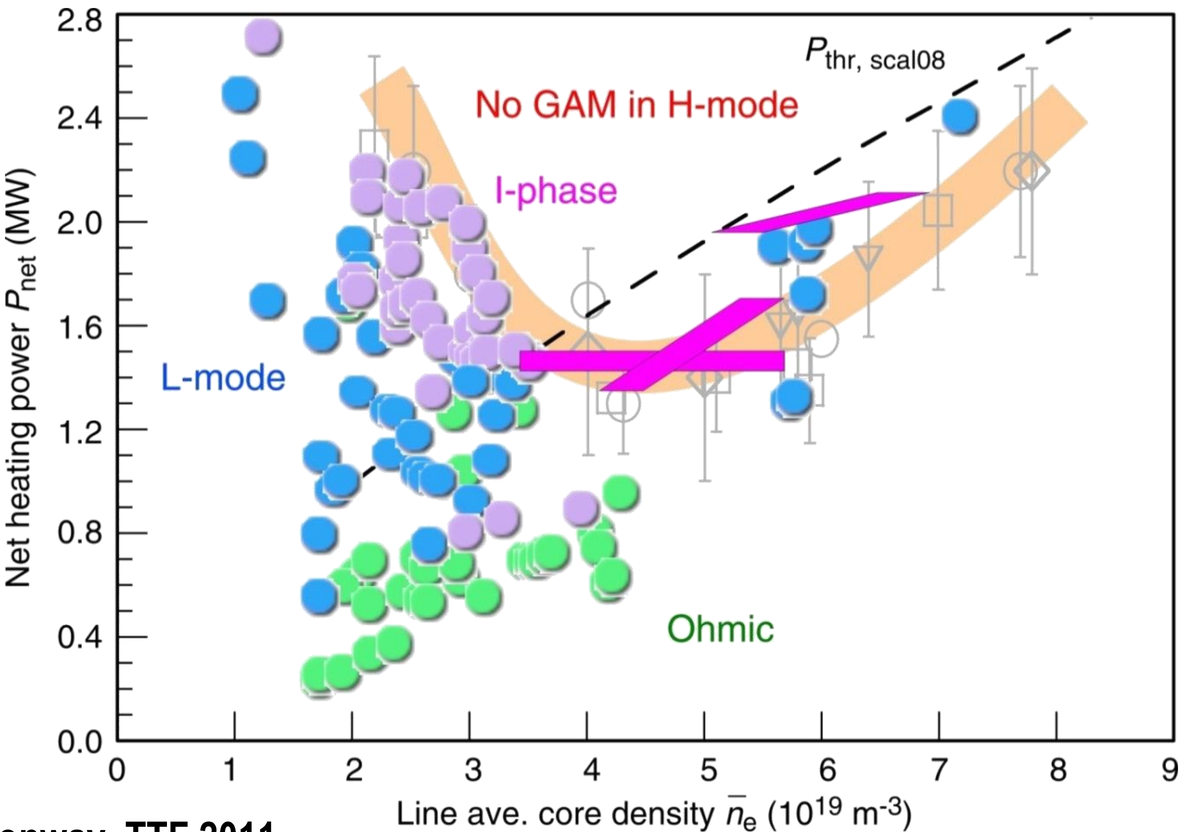

G. Conway, TTF 2011

- Decouple electron and ion channels: low density and ECRH

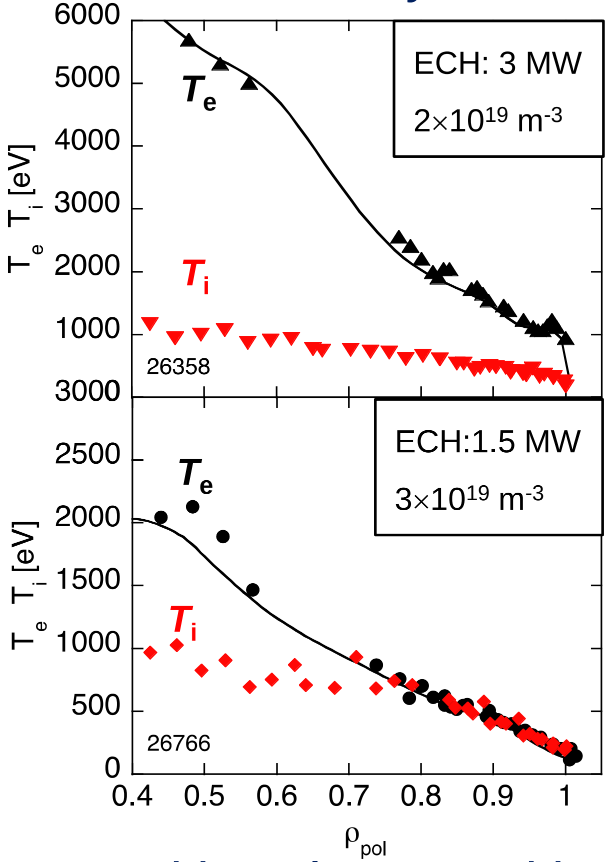

- Ion pressure gradient separates L and H-modes
- Simple neoclassical expression

$$E_r^{\text{neo},(0)} = \frac{\nabla p_i}{e n_i}$$

Stroth PPC 11

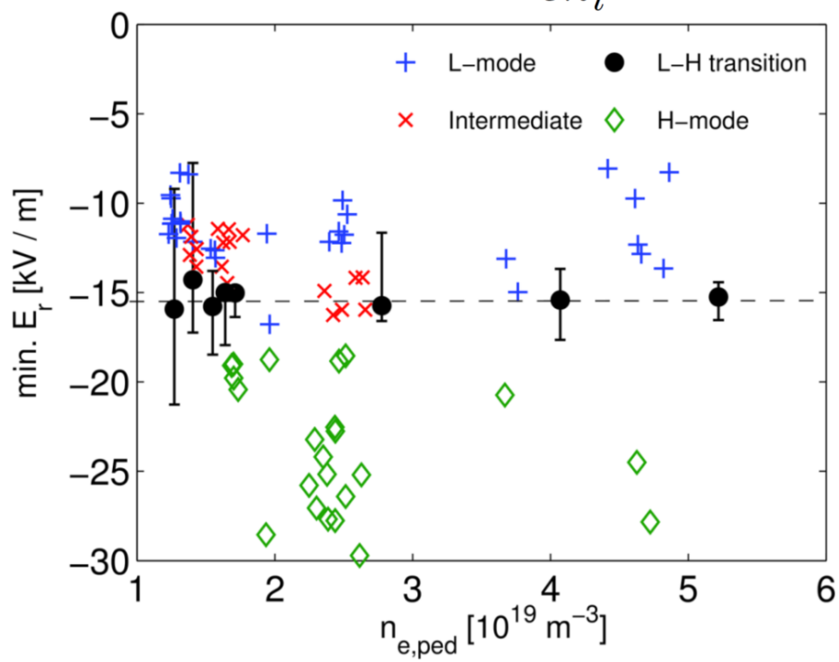

- L-H transition close to critical value of the radial electric field
- Increase of P_{thres} at low density due to reduced ion-electron coupling

P. Sauter NF 2012

F. Ryter EX/1-5

The edge radial electric field and neoclassical theory

- Radial electric field from CXRS

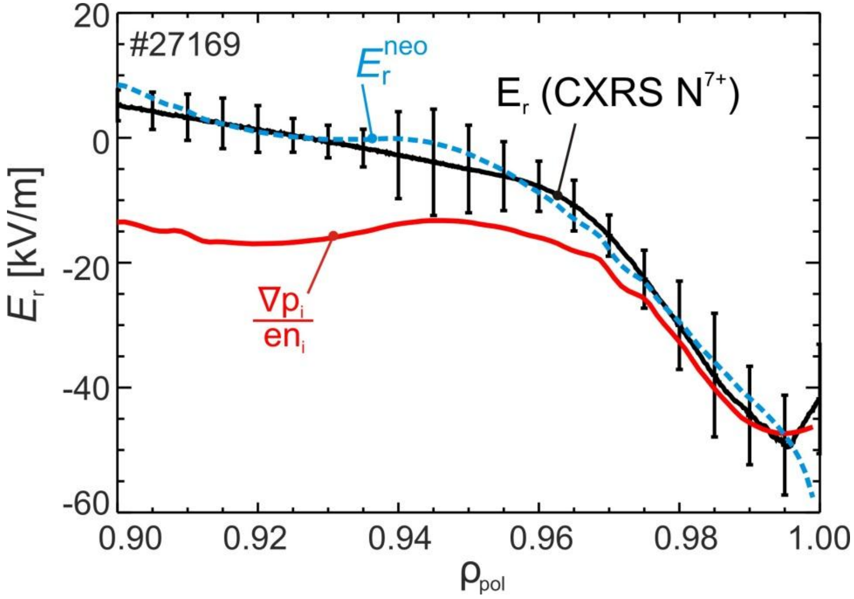

- Neoclassical E_r (NEOART) consistent with experiment
- In the edge simple expression without toroidal flow fits data

$$E_r^{\mathrm{neo},(0)} = \frac{\nabla p_i}{e n_i}$$

- Consistent CXRS data obtained from different impurities

$$E_r = -u_\theta B_\varphi + u_\varphi B_\theta + \frac{p'}{qn}$$

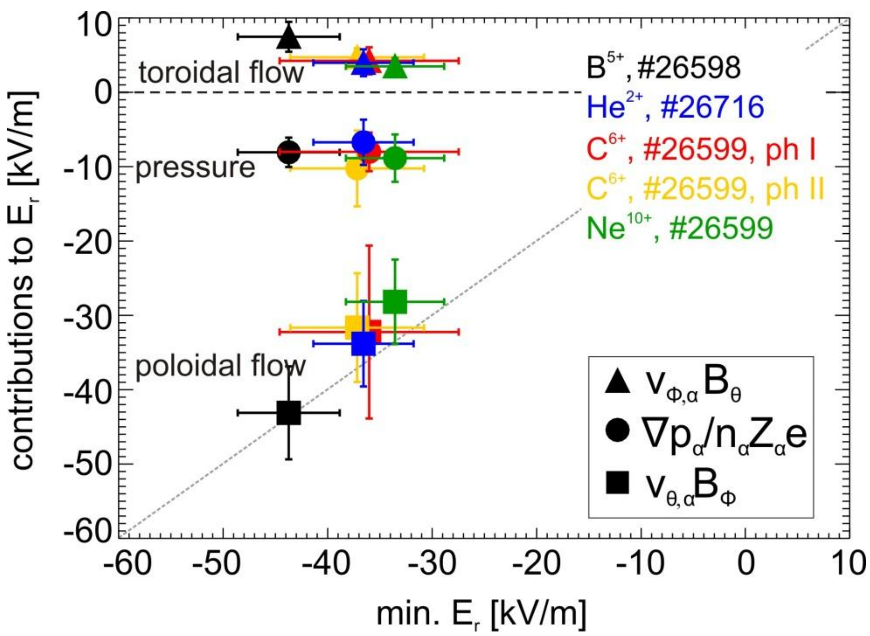

E. Viezzer NF submitted

SOL power-decay length scaling from AUG and JET

- Inter-ELM scaling from high-resolution IR camera data

$$\lambda_q = 0.73 \cdot B_{tor}^{-0.78} \cdot q_{cyl}^{1.20} \cdot P_{SOL}^{0.10} \cdot R_{geo}^{0.02}$$

(Carbon divertor, attached conditions, inter ELM)

- Extrapolation to ITER is 1 mm
- Consequences
  - divertor must be detached!
  - DEMO needs radiation from inside the separatrix
  - must be kept compatible with H-L threshold

- Scaling is consistent with model by Goldston

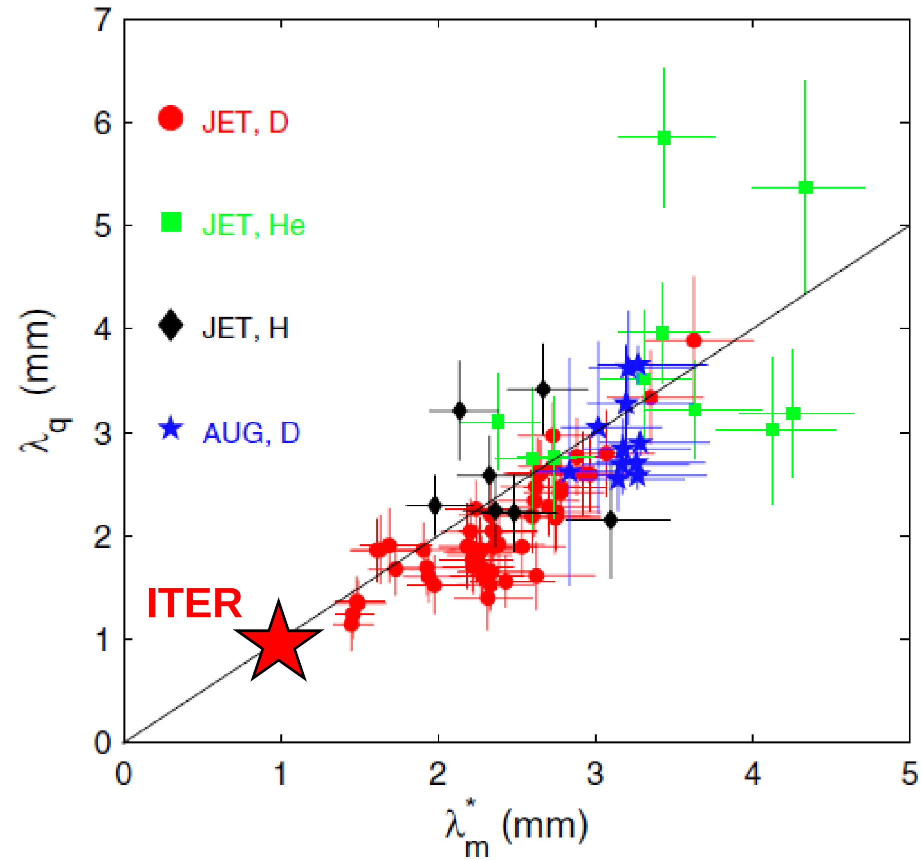

- Confirmed by multi-device study

T. Eich ITR/1-1

Increased power-decay length with radiative cooling

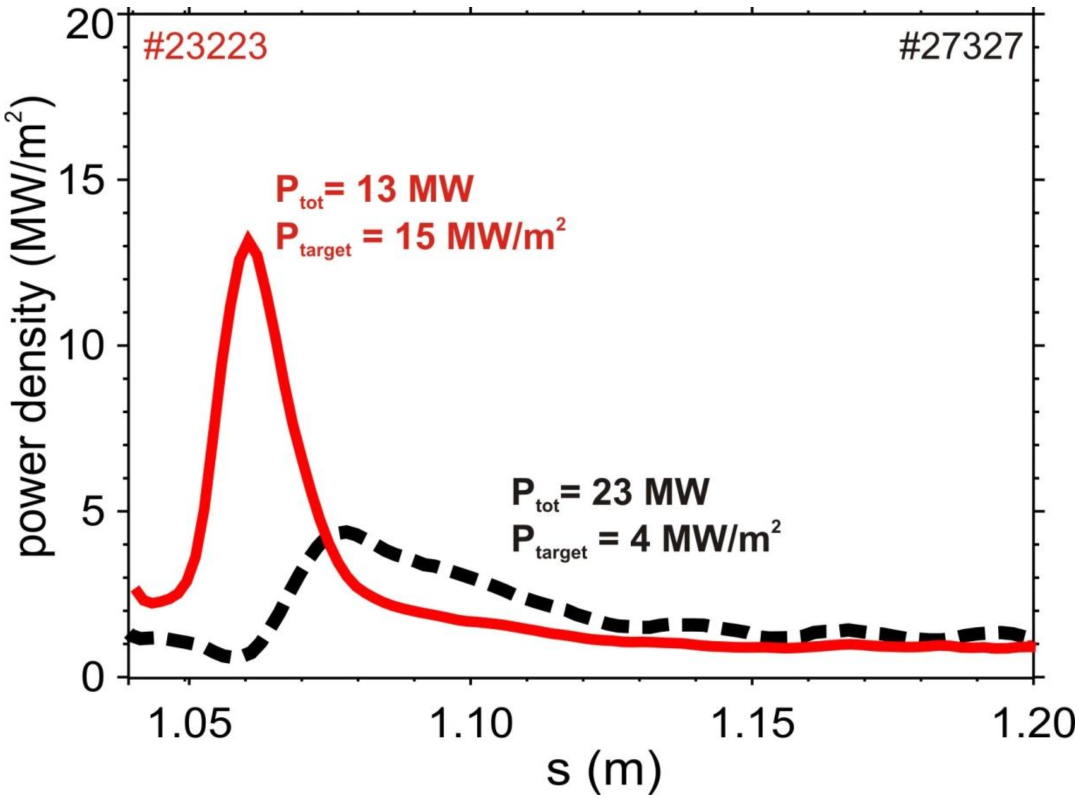

- Semi-detached conditions due to radiative cooling
- Deposition width increases from 2 to 5 cm
- Emphasizes the need to understand conditions for detachment

Experimental investigation of divertor detachment

- Insufficient understanding $\rightarrow$ no reliable predictions
- Unique diagnostic for 2D distribution of density (Stark broadening) and radiation (fast bolometry)

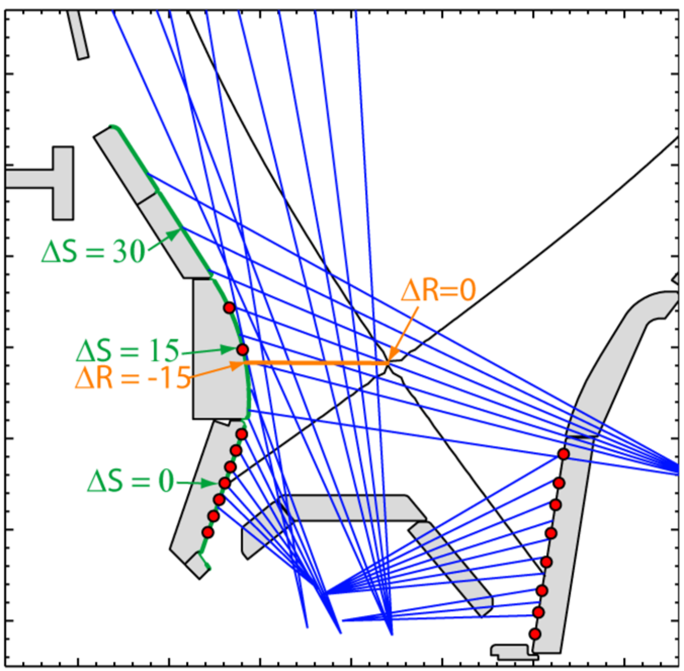

- Study density ramps in OH and L-mode discharges
- Detachment is observed to happen through three phases

S. Potzel PSI 2012

Three steps into divertor detachment

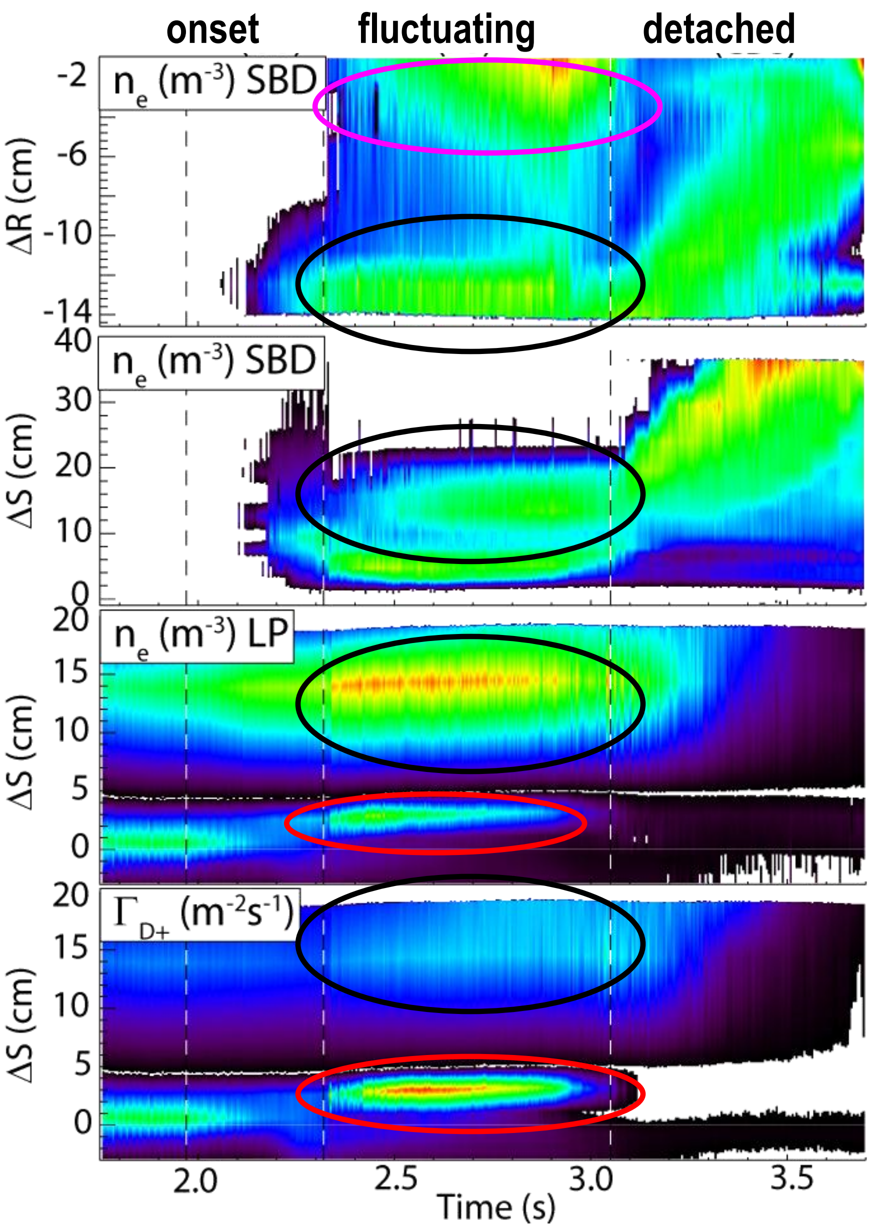

- High density in the inner divertor volume and the far SOL
- Density increase around x-point
- Fluctuations in 5 kHz range

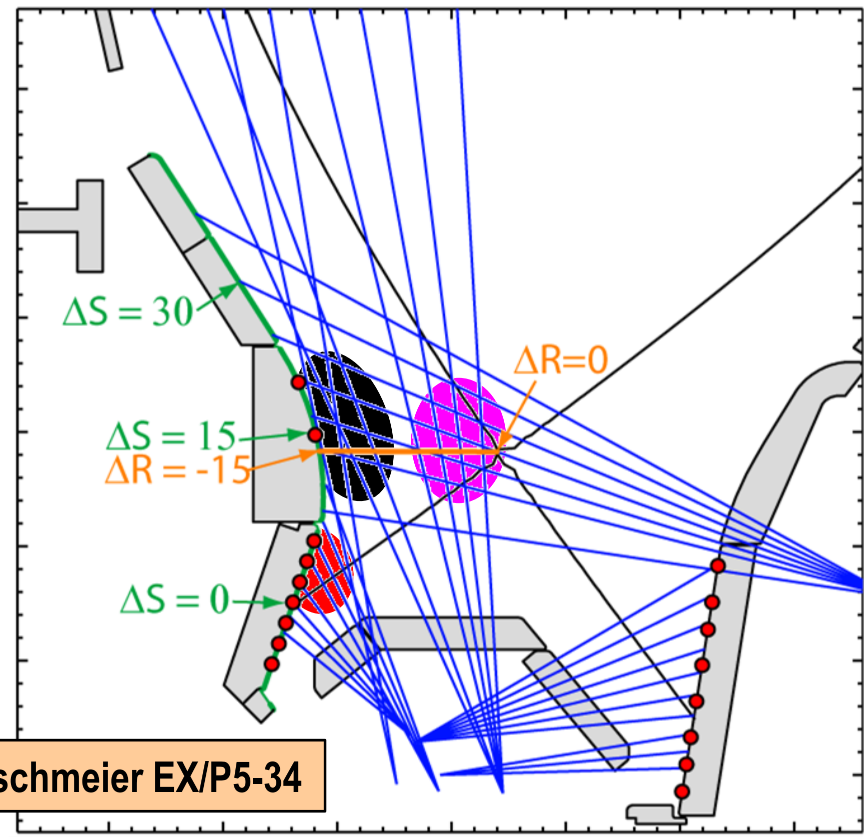

M. Wischmeier EX/P5-34

Three steps into divertor detachment

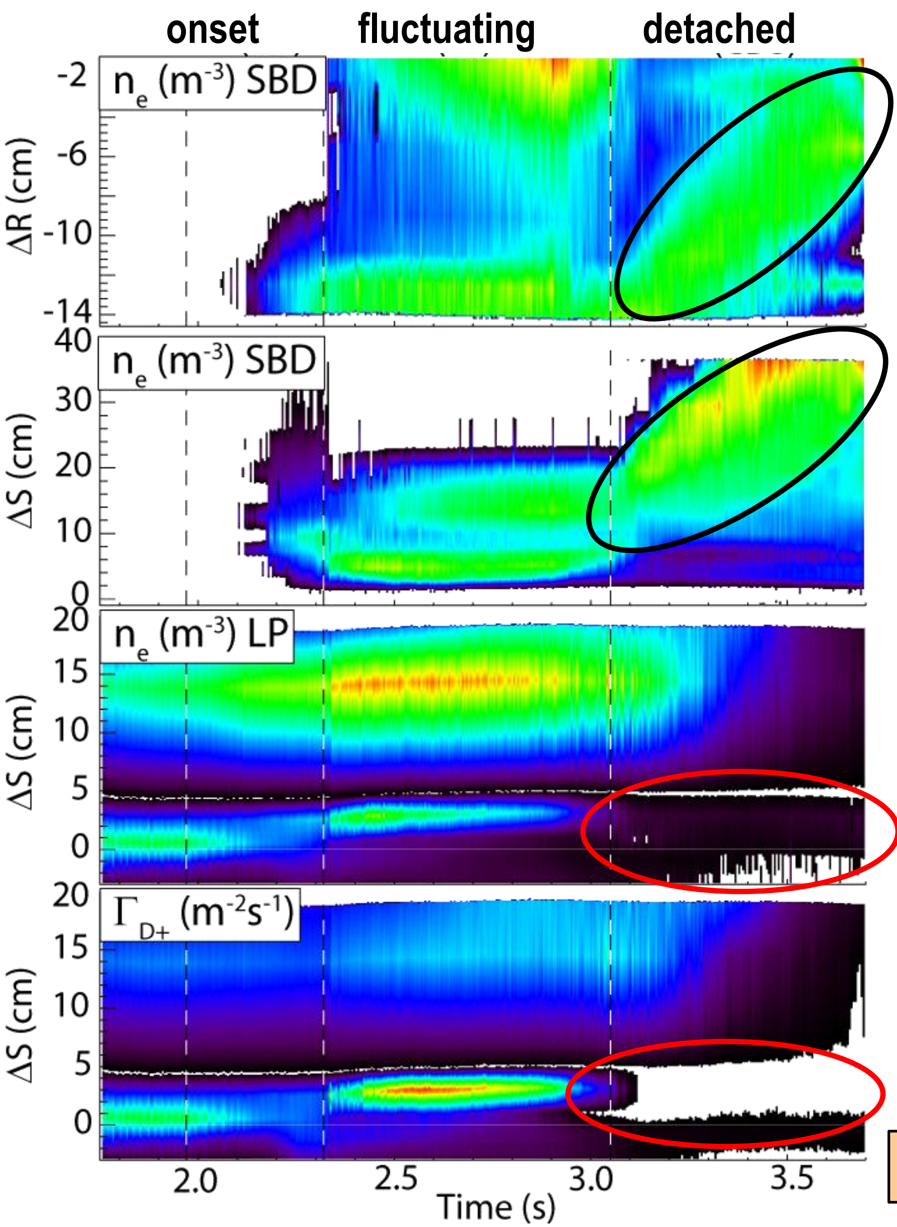

- Density drop at inner strike line
- Density front moves from target to x-point
- Outer divertor detaches

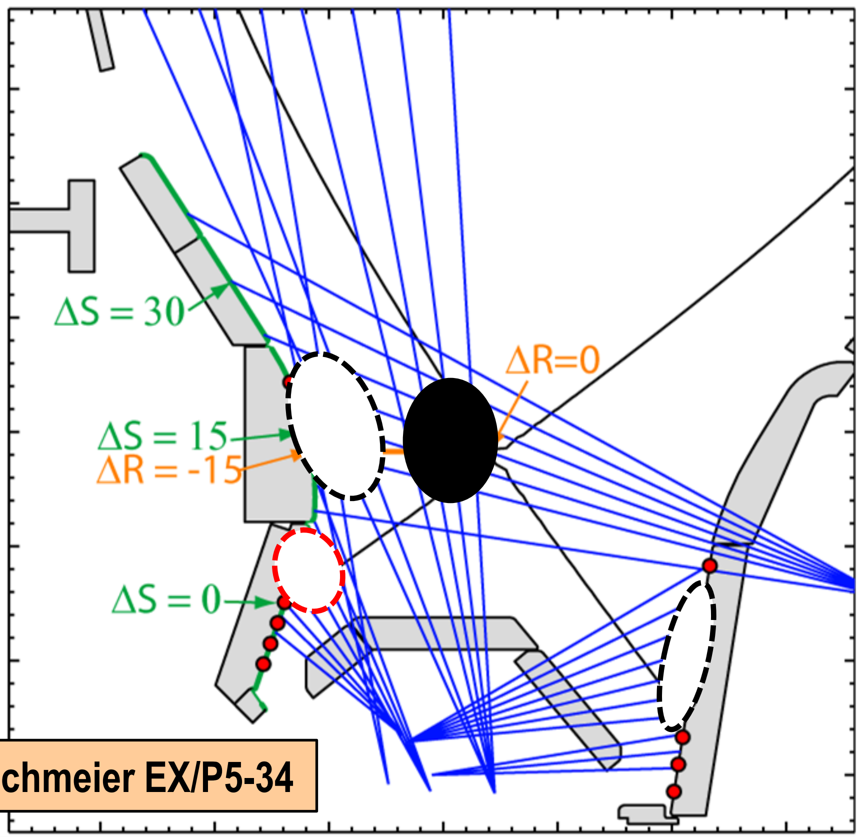

M. Wischmeier EX/P5-34

SOL turbulence from Langmuir probes and GEMR

- Plasma potential measured by two techniques (emissive, cond. sampling)

Experiment

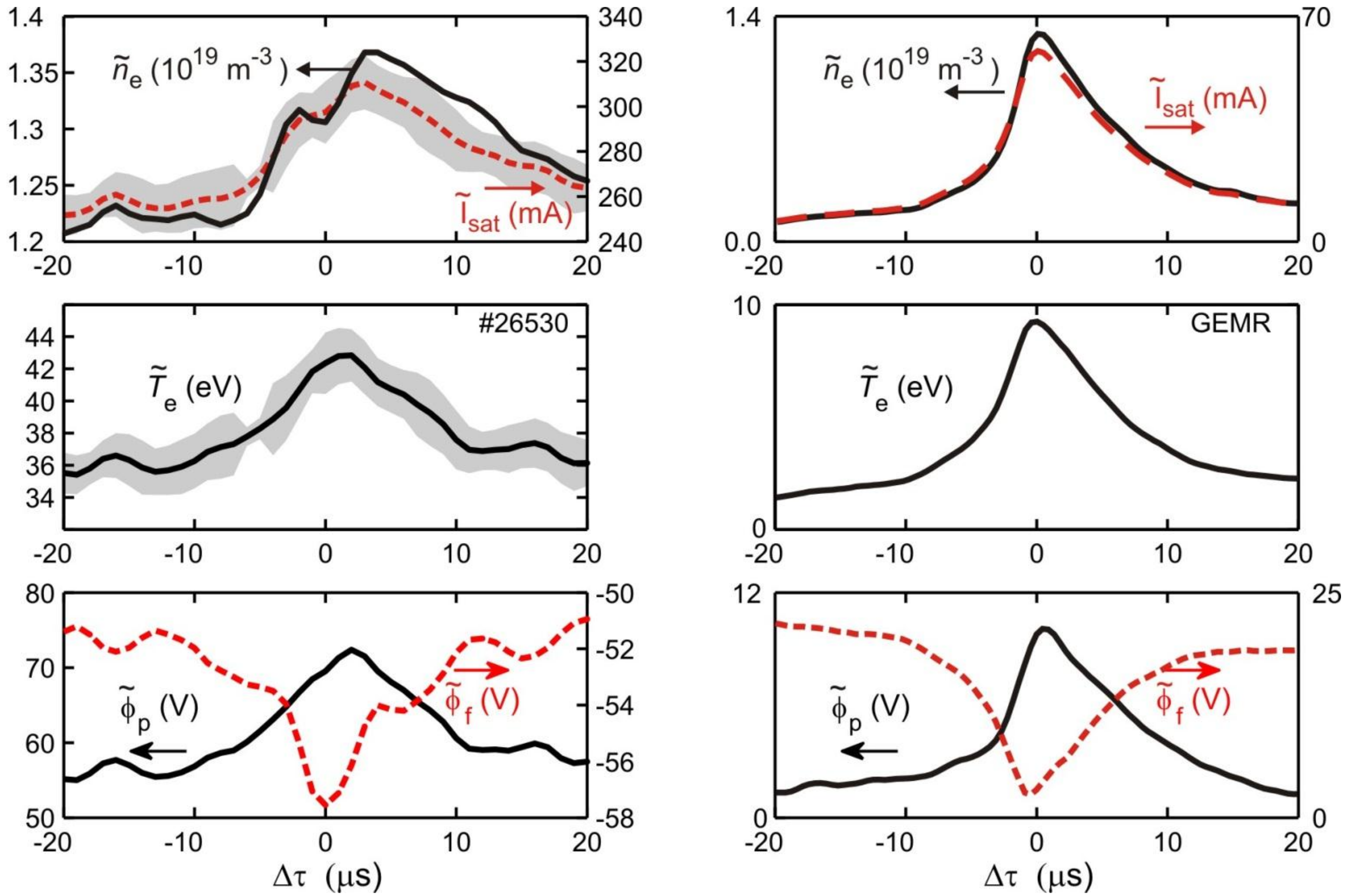

Gyro-fluid code GEM3

- All parameters are in phase → drift-wave turbulence
- Consistent with data from synthetic Langmuir probes in GEMR

B. Nold NJP 2011

M. Kočan EX/P7-23

First ion temperature measurements in the SOL

- Retarding field analyzer measures the ion temperature in turbulent and ELM filaments/blobs

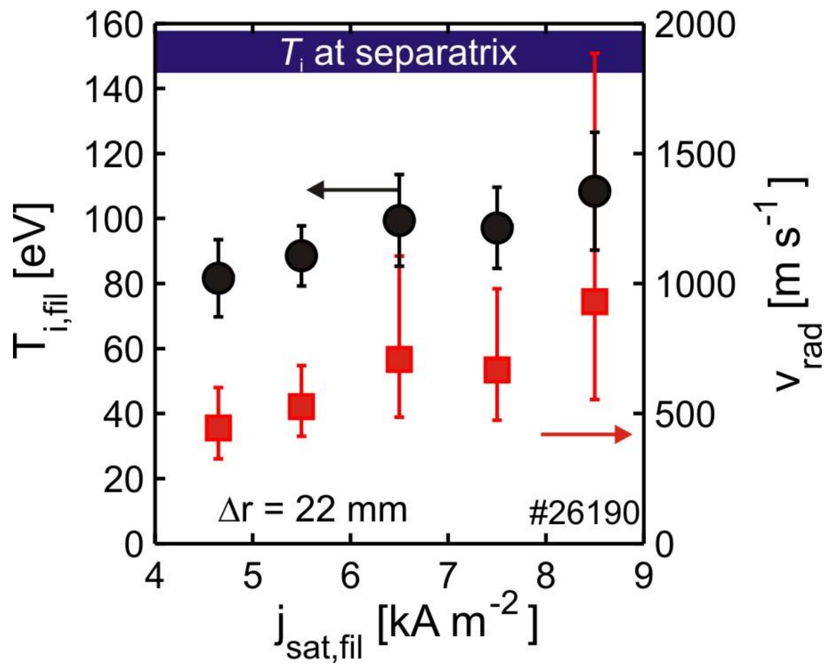

- The ion temperature
  - of up to 70 % of the pedestal value
  - increases with blob "density"

- Temperature in ELM filaments scales with ELM size

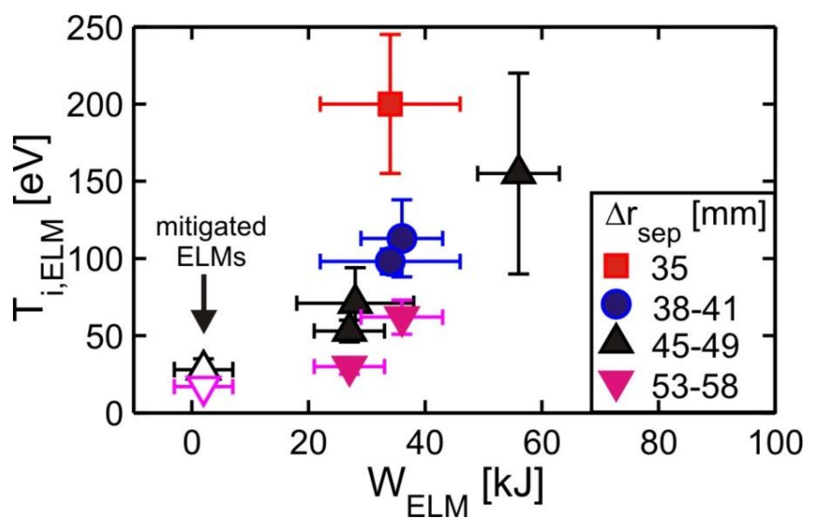

- With mitigated ELMs ions in blobs are colder

M. Kočan EX/P7-23

The ASDEX Upgrade Team (2011-12)

J. Adamek[1], L. Aho-Mantila[2], S. Äkäslompolo[2], C. Amdor[6], C. Angioni, M. Balden, S. Bardin[3], L. Barrera Orte, K. Behler, E. Belonohy, A. Bergmann, M. Bernert, R. Bilato, G. Birkenmeier, V. Bobkov, J. Boom[4], C. Bottereau[20], A. Bottino, F. Braun, S. Brezinsek[13], T. Brochard[11], M. Brüdgam, A. Buhler, A. Burckhart, F.J. Casson , A. Chankin, I. Chapman [8], F. Clairet[10], I.G.J. Classen[4], J.W. Coenen[13], G.D. Conway, D.P. Coster, D. Curran[17], F. da Silva[6], P. de Marné, R. D'Inca, M. Douai[10], R. Drube, M. Dunne[17], R. Dux, T. Eich, H. Eixenberger, N. Endstrasser, K. Engelhardt, B. Esposito[5], E. Fable, R. Fischer, H. Fünfgelder, J.C. Fuchs, K. Gal, M. Garcia Munoz, B. Geiger, L. Giannone, T. Görler, S. da Graca[6], H. Greuner, O. Gruber, A. Gude, L.Guimarais[6], S. Günter, G. Haas, A.H. Hakola[2], D. Hangan, T. Happel, T. Härtl, T. Hauff, B. Heinemann, A. Herrmann, J. Hobirk, H. Höhnle[10,] M. Hölzl, C. Hopf, A. Houben, V. Igochine, C. Ionita[12], A. Janzer, F. Jenko, M. Kantor, C.-P. Käsemann, A. Kallenbach, S. Kálvin[7], M. Kantor[13], A. Kappatou[4], O. Kardaun, M. Kaufmann, A. Kirk[8], H.-J. Klingshirn, M. Kocan, G. Kocsis[7], C. Konz, R. Koslowski[13], K. Krieger, M. Kubic[10], T. Kurki-Suonio[2], B. Kurzan, K. Lackner, P.T. Lang, A. Lazaros[23], P. Lauber, M. Laux, F. Leipold[14], F. Leuterer, S. Lindig, S. Lisgo[10], A. Lohs, T. Lunt, H. Maier, T. Makkonen, K. Mank, M.-E. Manso[5], M. Maraschek, M. Mayer, P.J. McCarthy[17], R. McDermott, F. Mehlmann[12], H. Meister, L. Menchero, F. Meo[14], P. Merkel, R. Merkel, V. Mertens, F. Merz, A. Mlynek, F. Monaco, S. Müller[19], H.W. Müller, M. Münich, G. Neu, R. Neu, D. Neuwirth, M. Nocente[15], B. Nold[10], J.-M. Noterdaeme, G. Pautasso, G. Pereverzev, B. Plöckl, Y. Podoba, F. Pompon, E. Poli, K. Polozhiy, S. Potzel, M.J. Püschel, T. Pütterich, S.K. Rathgeber, G. Raupp, M. Reich, F. Reimold, T. Ribeiro, R. Riedl, V. Rohde, G. v. Rooij[4], J. Roth, M. Rott, F. Ryter, M. Salewski[14], J. Santos[6], P. Sauter, A. Scarabosio, G. Schall, K. Schmid, P.A. Schneider, W. Schneider, R. Schrittwieser[12,] M. Schubert, J. Schweinzer, B. Scott, M. Sempf, M. Sertoli, M. Siccinio, B. Sieglin, A. Sigalov, A. Silva[6], F. Sommer, A. Stäbler, J. Stober, B. Streibl, E. Strumberger, K. Sugiyama, W. Suttrop, G. Tardini, M. Teschke, C. Tichmann, D. Told, W. Treutterer, M. Tsalas[4], M. A. Van Zeeland [9], P. Varela[6], G. Veres[7], J. Vicente[6], N. Vianello[16], T. Vierle, E. Viezzer, B. Viola[16], C. Vorpahl, M. Wachowski[12,] D. Wagner, T. Wauters[10], A. Weller, R. Wenninger, B. Wieland, M. Willensdorfer[18], M. Wischmeier, E. Wolfrum, E. Würsching, Q. Yu, I. Zammuto, D. Zasche, T. Zehetbauer, Y. Zhang, M. Zilker, H. Zohm

Max-Planck-Institut f. Plasmaphysik, EURATOM-Association, Germany
[1]Institute of Plasma Physics, Praha, Czech Republic
[2]Asscociation EURATOM-Tekes, Helsinki, Finland
[3]Institute of Atomic Physics, EURATOM Association-MEdC, Romania
[4]FOM-Institute DIFFER, EURATOM Association, The Netherlands
[5]C.R.E ENEA Frascati, EURATOM Association, Italy
[6]IPFN, EURATOM Association-IST Lisbon, Portugal
[7]KFKI, EURATOM Association-HAS, Budapest, Hungary
[8]EURATOM/CCFE Fusion Association, Culham Science Centre, UK,
[9]General Atomics, San Diego, California, USA
[10] Institut f. Plasmaforschung, Universität Stuttgart, Germany
[11]EFDA-JET, Culham, United Kingdom
[12] University of Innsbruck, EURATOM Association-ÖAW, Austria
[13]Forschungszentrum Jülich, Germany
[14]Association EURATOM - DTU, Roskilde, Denmark
[15]EURATOM Association-ENEA, IFP, CNR, Milano, Italy,
[16]Consorzio RFX, EURATOM Association-ENEA, Padova, Italy
[17]University College Cork, Association EURATOM-DCU, Ireland
[18]IAP, TU Wien, EURATOM Association-ÖAW, Austria
[19]Dept. Mech. & Aerospace Eng. UCSD, La Jolla, USA
[20]CEA, Cadarache, France
[21]Institut Jean Lamour, UMR 7198 CNRS, Vandoeuvre, France
[22] Warsaw Univ. of Technology, Warsaw, Poland
[23] Association EURATOM/Hellenic-Republic, Athens, Greece

Summary of ASDEX Upgrade Results

- Record P/R values (14 MW/m) achieved with power loads < 5 MW/m^2
- Robust ELM mitigation at high densities without loss of confinement
- Enhanced pellet fuelling and $n = 1.6 n_{GW}$ in ELM mitigated discharges
- L-H transitions happen at critical value of the ion pressure gradient and E_r
- Radial electric field consistent with neoclassical theory
- Power decay length at divertor entrance independent of major radius
- High density region and fluctuations in inner divertor before detachment
- Turbulence in the near SOL consistent with drift waves and simulations
- High ion temperatures measured in the far SOL
- ECRH modifies core particle and momentum transport
- Rotation profiles reproduced by residual stress from linear gyro-kinetic calc.
- Fast-particle slowing down and diffusion are classical